Steam cracking in a semi-industrial dual fluidized bed reactor: Tackling the challenges in thermochemical recycling of plastic waste

N.B. When citing this work, cite the original published paper.

(article starts on next page)

Steam cracking in a semi-industrial dual fluidized bed reactor: Tackling the challenges in thermochemical recycling of plastic waste

Chahat Mandviwala [*], Renesteban Forero Franco [*], Teresa Berdugo Vilches, Ivan Gogolev, Judith González-Arias, Isabel Cañete Vela, Henrik Thunman, Martin Seemann

Department of Space, Earth and Environment (SEE), Division of Energy Technology, Chalmers University of Technology, 412 96 Gothenburg, Sweden

ARTICLE INFO

ABSTRACT

Steam cracking is an integral process in the plastic manufacturing industry. Conventional steam crackers are tubular reactors and use fossil-based feedstocks like naphtha and LPG. This work presents steam cracking in a dual fluidized bed (DFB) reactor as an alternative for the direct steam cracking of plastic waste. Experiments were performed on a semi-industrial DFB system using naphtha, clean polyolefins, real-life plastic wastes, and a polyolefin-derived pyrolysis oil. The results show that steam cracking in a DFB is fundamentally equivalent to steam cracking in tubular reactors. Selective production of light olefins and monoaromatics was achieved within a temperature range of 700–825 °C. Naphtha yielded up to 56 % light olefins and 7 % BTXS, with ethylene and BTXS production positively correlating with cracking severity, while C3 and C4 olefins show a negative correlation. These results confirm that the established steam cracking mechanisms also apply to large-scale DFB steam crackers. The yield of light olefins is consistently obtained at approximately 52 % relative to the polyolefin content of the feedstock, regardless of the non-polyolefin content. This highlights the DFB steam cracker's ability to produce light olefins directly from plastic waste without presorting. However, steam cracking in DFB results in significantly higher CO and CO_2 yields than conventional steam cracking, especially with feedstocks containing non-polyolefins like PET and cellulose. Additionally, steam cracking of an olefin-rich pyrolysis oil yields up to 50 % light olefins with minimal coke formation, highlighting the potential in processing plastic waste pyrolysis oils without pretreatment steps such as distillation and hydrotreatment.

1. Introduction

Steam cracking is central to the plastic manufacturing industry and is crucial for producing most plastic materials [1,2]. In this process, fossil hydrocarbons such as naphtha, liquefied petroleum gas (LPG), or ethane are rapidly heated in tubular reactors and broken down into smaller molecules. The primary products of the steam cracking process include ethylene, propylene, butenes, benzene, toluene, and xylene, which are molecular building blocks or monomers of a wide range of plastic materials [3,4]. A steam cracker has a downstream gas separation unit that separates the product stream into individual monomers for subsequent polymerization into various plastics [5].

Increasing environmental concerns and the finite nature of fossil resources have driven the need for innovative waste management and recycling strategies to achieve a circular economy [6]. This shift is critical for the plastic industry, which relies heavily on fossil resources, accounting for up to 6 % of global fossil consumption [7,8]. The linear usage of plastic materials, characterized by a take-make-dispose model, adds to the complexity of this sustainability problem [8]. In light of these concerns, there is a pressing need for recycling technologies that bridge the gap between waste management and sustainable production of plastic materials [9].

Among different recycling methods for plastic materials, thermochemical recycling has attracted significant attention due to its focus on recovering the monomers of plastics, which can be used to manufacture new plastics of virgin quality [6]. This characteristic gives

thermochemical recycling an edge over mechanical recycling, which has a limited ability to produce high-quality recycled materials. The inherent properties of plastics also constrain the number of times they can be mechanically recycled. Consequently, while mechanical recycling may apply to some well-sorted plastic wastes, thermochemical recycling methods will be crucial in achieving a circular economy for plastic materials [10].

Thermochemical recycling processes have been extensively researched for polyolefins because they are among the most important and widely used plastics [11,12]. The extensive use of polyolefins in the packaging industry has made them the predominant single-use materials. Consequently, polyolefins account for up to 60 % of the plastic waste worldwide [10]. Thermochemical recycling of polyolefins aims to break down the molecular structure of polyolefins to produce their constituent monomers. Specifically, thermochemical recycling of polyolefins aims to selectively produce light olefins (C2–C4) such as ethylene, propylene, and butadiene, along with monoaromatics such as benzene, toluene, xylenes, and styrene (BTXS) [9,11]. These monomers can polymerize again to produce a range of polyolefins like polyethylene (PE) and polypropylene (PP) or other polymers such as polyvinyl chloride (PVC) and polyethylene terephthalate (PET).

Conventional steam crackers, currently used for producing light olefins and monoaromatics, cannot be directly employed for the thermochemical conversion of solid feedstocks like polyolefins or other polymers [7]. This limitation arises from the inherent design of tubular steam crackers, which are suitable only for converting liquid or gaseous hydrocarbon feedstocks like naphtha and LPG [13]. Additionally, the heterogeneous nature of plastic waste imposes heat transfer limitations on a tubular steam cracker. To address these challenges, researchers have proposed various solutions over the years. One such approach involves converting plastic waste into a naphtha-like drop-in feedstock for steam cracking, thereby replacing fossil feedstocks with recycled resources [11]. Additionally, significant research has focused on replacing conventional steam crackers with alternative cracking processes capable of handling solid plastic waste [10].

In producing recycled feedstocks for the steam cracking process, polyolefin pyrolysis has gained the most interest recently. This process focuses on producing liquid hydrocarbons from polyolefins, achievable through various methods such as employing different heating rates, using diverse environments (hydrogen, steam, oxidative, and inert), and utilizing different reactor systems like fluidized beds, fixed beds, and rotary kilns [14–17]. The liquid hydrocarbon products of pyrolysis, commonly known as pyrolysis oils, are envisioned as feedstock for the steam cracking process to produce light olefins and monoaromatics [18]. In this scheme, pyrolysis oils will replace fossil-based naphtha, providing a more sustainable solution.

Despite the potential of pyrolysis for the thermochemical recycling of polyolefins, its industrial-scale development faces several challenges. Pyrolysis oils derived from polyolefins contain significantly longer hydrocarbon chains and higher olefin content than naphtha [19,20]. Moreover, pyrolysis oils contain a wide range of hydrocarbon chain lengths (C5 to C30) and often include heteroatoms such as oxygen, nitrogen, sulfur, and chlorine, which are problematic for conventional steam crackers. These components can exacerbate coking issues in steam crackers, necessitating frequent decoking and reducing production efficiency. In mitigating these challenges, pyrolysis oils often require distillation and hydrotreatment to obtain a naphtha-like product with shorter hydrocarbon chains and reduced olefin content. Removing non-polyolefin content from plastic waste is also essential to lower the heteroatom content in pyrolysis oil [20–22]. However, the costs associated with presorting and hydrotreatment make it difficult for pyrolysis oils to compete with fossil naphtha despite the technical feasibility of the pyrolysis process.

Additionally, from the standpoint of achieving circular utilization of plastics, the pyrolysis process has limitations in delivering complete recyclability of plastic waste streams. The requirement to produce naphtha-like pyrolysis oil will result in some plastic waste fractions getting rejected. These rejected fractions will likely get incinerated if not recycled by other methods, complicating the goal of complete recyclability.

In recent years, researchers have also explored the selective production of light olefins and BTXS directly from plastic waste through various catalytic cracking processes [23–25]. These processes can also convert untreated pyrolysis oils into light olefins, eliminating the need for an additional hydrotreatment step after the pyrolysis process [26,27]. A catalytic cracking process for producing paraffinic liquid hydrocarbons from plastic waste could also be an attractive solution. The obtained paraffinic hydrocarbons can be further processed into light olefins and BTXS in conventional steam crackers. This thermochemical route involves hydrocracking or hydropyrolysis of plastic waste.

The primary drawback of catalytic cracking processes is catalyst deactivation. This deactivation occurs because plastic waste contains numerous impurities, such as nitrogen, sulfur, and alkali metals, which poison the catalysts [28–30]. Therefore, ensuring thorough pretreatment and purification of the plastic waste feed is essential to extend the catalyst's lifetime. Continuous or frequent catalyst regeneration is crucial to maintain conversion efficiency [28]. The cost of catalysts poses a significant barrier to the economic feasibility of the catalytic cracking processes.

Gasification is another widely studied thermochemical recycling process that partially oxidizes plastic waste to produce syngas [31,32]. This process operates at high temperatures, typically from 700 to 1000 °C, effectively breaking down the molecular structure of polymers into syngas (CO, CO_2, H_2, and CH_4) [31,32]. Syngas produced in this manner can be selectively converted into light olefins through synthesis processes like Fischer-Tropsch (FT) and Methanol-to-Olefins (MTO) [33,34]. Gasification is typically non-catalytic and uses pure oxygen, steam, or air as the gasifying agent. The elevated temperatures used in gasification allow for the conversion of various types of plastic waste without extensive presorting or pretreatment [35].

Gasification stands out as a versatile recycling process with the potential to achieve complete recyclability of plastic waste. Despite its promise, several factors make it economically unattractive. One primary concern is the substantial energy demand required to produce syngas from plastic waste. This high energy requirement increases operational costs, thereby diminishing the economic viability of the recycling process [7,22]. Another crucial issue is the necessity for additional hydrogen in downstream synthesis processes. This hydrogen is essential for converting the CO_2 generated from oxygen-containing polymers during gasification into the required monomers [7].

Pyrolysis, catalytic cracking, and gasification show potential for recycling plastic waste. However, their industrial-scale development faces numerous challenges that hinder the complete recyclability of plastics. A significant barrier is the inadequacy of conventional steam crackers, which struggle with direct steam cracking of solid plastic waste for selectively producing light olefins and monoaromatics. Addressing these challenges necessitates a transformation in steam cracking technology, requiring a more robust reactor configuration capable of processing a variety of feedstocks, including unsorted plastic wastes and untreated pyrolysis oils.

The dual fluidized bed (DFB) reactor has recently emerged as a promising option for the thermochemical recycling of plastic waste to overcome the limitations of conventional steam crackers and catalytic cracking while selectively producing desired monomers from plastic waste [36]. Wilk et al. first tested thermochemical recycling in a DFB, demonstrating the selective production of light olefins and monoaromatics from polyolefin-rich feedstocks [37]. Thunman et al. validated this approach in a semi-industrial DFB system, showcasing its scalability [7]. Fig. 1 summarizes the three thermochemical recycling routes discussed so far, along with the proposed route in this work, which involves direct steam cracking of unsorted plastic waste in a DFB reactor.
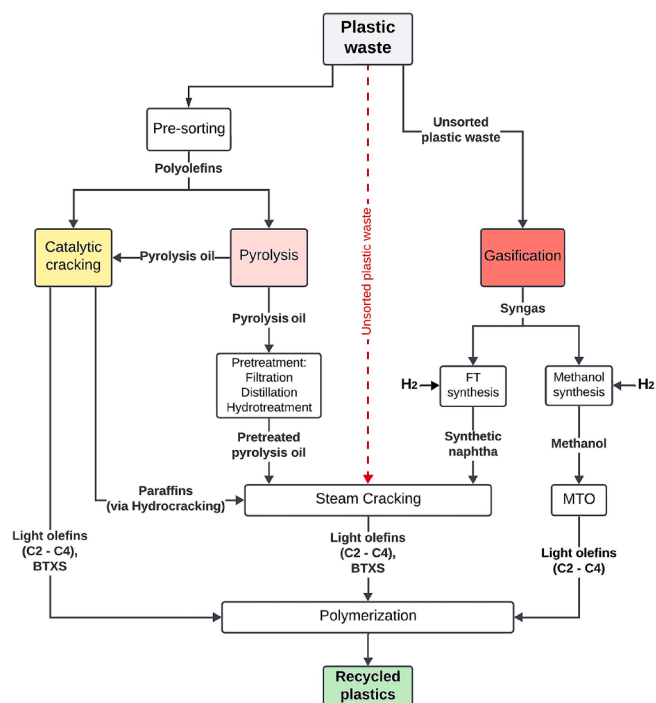
Fig. 1. The most commonly explored and envisioned thermochemical routes for the recycling of plastic waste. The thermochemical processes include pyrolysis, gasification, and catalytic cracking. The process flow indicated by the dashed line represents direct steam cracking of unsorted plastic waste, the thermochemical route proposed in this work.

This work aims to establish that steam cracking in a DFB is equivalent to steam cracking in tubular reactors by processing naphtha in a semi-industrial DFB steam cracker and showing that the conversion and product distribution closely resemble those in conventional steam crackers. This work also demonstrates the effectiveness of the DFB steam cracking process in converting unsorted plastic waste streams such as mixed packaging waste. Herein, we show that the process eliminates the need to separate the polyolefin content of waste streams by selectively producing light olefins in proportion to the polyolefin content. We also show how the non-polyolefin content of the waste stream gets converted in the DFB steam cracking process. Furthermore, we present a superior capability of DFB reactors over tubular reactors in continuously removing solid carbon during steam cracking, eliminating the need for intermittent decoking. This capability allows processing feedstocks prone to coke formation, such as pyrolysis oils, without distillation and hydrotreatment. The results also highlight the DFB steam cracker's effectiveness in handling high-ash plastic waste, making it suitable for processing waste streams like automotive shredder residue and cable plastics. The experimental campaign spanned over five years, with the reactor system operating continuously from November to April each year. During this period, over 200 h were dedicated to the steam cracking of six different feedstock. These results highlight the scalability and continuous operation capabilities of the process.

2. Materials and method

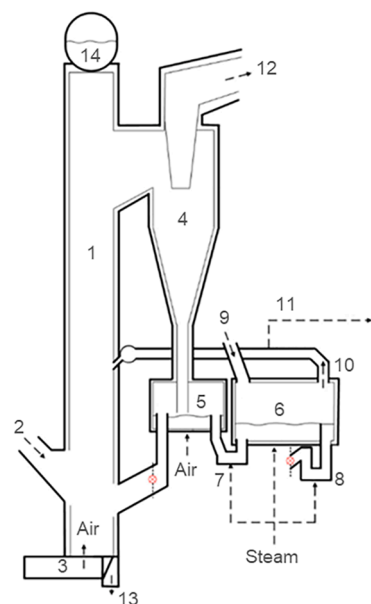### 2.1. The Chalmers DFB reactor

The semi-industrial DFB system at Chalmers University of Technology consists of a circulating fluidized bed (CFB) reactor interconnected with a bubbling fluidized bed (BFB) reactor. The CFB is a biomass boiler that provides indoor heating for the university campus. It has a cross-sectional area of 2.25 m^2, a height of 13.6 m, and a capacity of 12 MW$_{th}$. The BFB has a cross-sectional area of 1.44 m^2, a height of 1.6 m,

and a feedstock processing capacity of 4 MW$_{th}$, equivalent to 350 kg/h of naphtha or PE. The typical operating conditions include temperatures of 700–825 °C in the BFB and 780–850 °C in the bottom bed of the CFB, maintained at a sub-atmospheric pressure of 1–2 kPaG. Fig. 2 provides a simplified illustration of the DFB system.

In this setup, the CFB (labeled as #1 in Fig. 2) functions as a furnace for the boiler. The bed material circulates through a cyclone separator (#4) and a particle distributor (#5). For standard boiler operation, all the bed material is redirected back to the CFB. The CFB and the particle distributor are fluidized with either air or a combination of air and flue gases.

In DFB mode, part of the bed material is transferred to the BFB (#6) through a loop seal (#7) with a cross-sectional area of 0.05 m^2. The bed material returns to the CFB through a second loop seal (#8), as shown by the red symbols in Fig. 2. The loop seals and the BFB are fluidized with steam. The loop seals use a minimum of 35 kg/h of steam to prevent defluidization and gas leakage from the CFB side, while the BFB operates with a steam flow of 100–200 kg/h, with a fluidization number (u/u$_{mf}$) of 3 to 10. For further details on the fluidization regimes and the hydrodynamics of the Chalmers DFB system, refer to the works of Larsson et al. [38,39]. The DFB system functions simultaneously as an energy converter and a thermochemical reactor. Combustion occurs in the CFB using air, while thermochemical conversion occurs in the BFB in a steam environment. The exothermic reaction in the CFB supplies the heat needed for the endothermic thermochemical conversion in the BFB.

The CFB is fueled with wood chips or pellets through a fuel chute (#2), while the BFB can process solid and liquid feedstocks, such as plastic waste and naphtha. The feedstock for the BFB is introduced near loop seal 1, as shown in Fig. 2 (#9). The feeding process for solid feedstocks involves introducing them in molten form through an extruder. The extruder isolates the BFB from atmospheric air and maintains a controlled environment in the reactor. The extruder has a

1. CFB Reactor	8. Loop Seal 2
2. Feeding (CFB)	9. Feeding (BFB)
3. Wind Box	10. Product Gas Line
4. Cyclone Separator	11. Sampling Point
5. Particle Distributor	12. Flue Gas
6. BFB Reactor	13. Bottom Ash Removal
7. Loop Seal 1	14. Boiler

Fig. 2. Schematics of the semi-industrial DFB system at Chalmers University of Technology. The DFB system consists of a circulating fluidized bed (1) and a bubbling fluidized bed reactor (6). Adapted from the work performed by Larsson et al. [40].

maximum screw speed of 150 rpm and provides 135 kg/h throughput of PE. It has eight heating zones and provides a melt temperature of up to 350 °C. The extruder outlet is approximately 0.5 m above the bed material surface and feeds directly onto the top of the fluidized bed. Liquid feedstocks are introduced through a liquid injection port, located about 0.3 m above the fluidized bed, using a centrifugal pump. Fig. 3 shows a top view of the BFB, illustrating the two feeding points and the bed material flow.

The configuration of the fluidization nozzles in Fig. 3 is an approximate representation. The extrusion and liquid injection points are marked by a red and green dot, respectively. Three thermocouples are immersed in the fluidized bed. Thermocouple T1 measures the temperature of the bed material before it enters the BFB reactor. T2 measures the temperature after the bed material contacts the feedstock, and T3 measures the temperature just before the bed material exits the reactor. The bed material circulation through the BFB reactor can be adjusted within the range of 6 to 25 t/h, corresponding to a mass flux of 35 to 140 kg/m^{2}s through loop seal 1.

The product gas obtained from the BFB is directed to the furnace through the product gas line, as illustrated by #10 in Fig. 2. Since this facility primarily serves as a research site, there are no gas processing units associated with it, and therefore, the product gas undergoes combustion in the CFB. Any unconverted feedstock leaves the BFB with the bed material and gets combusted in the CFB.

2.2. Comparative features of the Chalmers DFB reactor and conventional steam crackers

The DFB configuration ensures the physical separation of the combustion and thermochemical reactions, preventing the mixing of product gas with air or flue gases. A similar physical separation is employed in conventional steam crackers, where reactor tubes are placed inside a furnace. In this setup, fossil feedstocks are cracked inside the tubes while combustion outside provides the required heat. The heat from combustion is transferred to the reactor tubes via radiation and conduction to the tube walls [40]. Due to these similarities, the conditions observed in a conventional steam cracker can be replicated in a DFB. The BFB creates a reaction environment like inside a steam cracker tube, while

Fig. 3. Top view schematic of the BFB reactor of the Chalmers DFB system.

1. Cyclone separator
2. Thermocouple (T1)
3. Particle distributor
4. Bed material from the particle aadistributor
5. Loop seal 1
6. Feeding point (Extruder)
7. Feeding point (Liquid injection)
8. Thermocouple (T2)
9. Fluidization nozzle
10. Thermocouple (T3)
11. Loop seal 2
12. Bed material to the boiler

the CFB supplies the necessary heat for the cracking reactions. Fig. 4 illustrates simplified schematics of a conventional steam cracker and a DFB steam cracker.

An analogy in the cracking temperature can be drawn between the Chalmers DFB and a conventional steam cracker based on the positions of the feedstock inlet and the three thermocouples (see Fig. 3). Temperatures T1 and T2 are equivalent to coil inlet and outlet temperatures of a conventional steam cracker, respectively. The coil outlet temperature (COT) is a critical process parameter in conventional steam crackers [2]. In this work, the temperature measured by thermocouple T2 is used to evaluate the cracking temperature. T2 reflects the temperature of the bed material after it has come into contact with the feedstock.

The short residence times achieved in conventional steam crackers can also be achieved in a DFB steam cracker. The on-bed feeding is expected to limit the contact time between the feedstock and the bed material. Additionally, the bubbling regime of the BFB limits heat transfer between the bed material and the product gas above the fluidized bed, restricting secondary cracking reactions [41].

An advantage of the DFB configuration over tubular reactors is its ability to continuously remove carbon deposits, commonly known as coke, formed during steam cracking. The bed material can also remove solid inorganic contaminants present in plastic waste. In the Chalmers DFB steam cracker, the carbon deposits are removed along with the bed material and combusted in the CFB (see Fig. 4). This process eliminates the need for intermittent decoking procedures, enabling uninterrupted operation.

The Chalmers DFB operates with bed materials derived from natural ores. A significant challenge with using natural ores in a DFB is the presence of species that undergo oxidation and reduction between the two reactors. The species include transition metal oxides and alkali metals. Additionally, in the Chalmers DFB, these species accumulate in the bed material due to biomass combustion in the CFB [42]. This process induces a higher oxidizing environment than a conventional steam cracker, promoting the formation of carbon oxides.

While the accumulation of these species is avoidable using tailored bed materials and clean feedstocks, this is difficult when using waste streams with unknown ash content. To minimize the oxidizing environment, Pissot et al. proposed a pre-reduction of the bed material [43]. The pre-reduction of bed material can be performed in the particle distributor (#5, Fig. 2) of the Chalmers DFB; however, it has never been tested before. Therefore, the product distribution obtained in this work is expected to contain higher amounts of carbon oxides than a conventional steam cracker.

2.3. Sampling and analytics

Two parallel slipstreams of the product gas, each approximately 10 l$_n$/min, are continuously extracted for sampling from the product gas line (see 11, Fig. 2). A hot filter, maintained at 350 °C, is positioned at the sampling point to ensure no solid particles get collected in the samples. One slipstream is for measuring individual species within the product gas mixture. The other slipstream is directed towards a high-temperature reactor (HTR) operating at 1700 °C, which decomposes the product gas into CO, CO_2, and H_2. These decomposition products are monitored online to calculate the elemental flows of C, H, and O exiting the steam cracker, according to the method developed by Israelsson et al. [44]. Sampling from both slipstreams simultaneously validates the carbon balance closure during stable operation. Table 1 summarizes the different sampling and measurement techniques applied to the two slipstreams.

The GC analyses performed on the samples collected from the two slipstreams provide the volumetric concentrations of the species listed in Table 1 in the product gas. A tracer approach is employed to determine the absolute yield of the individual species in the product mixture. In this method, a small flow (~35 ln/min) of high-purity helium (He) is introduced into the steam cracker along with the steam. The He flow is
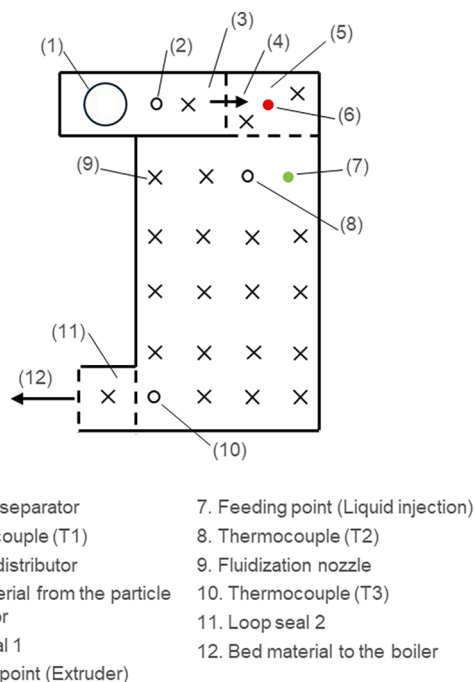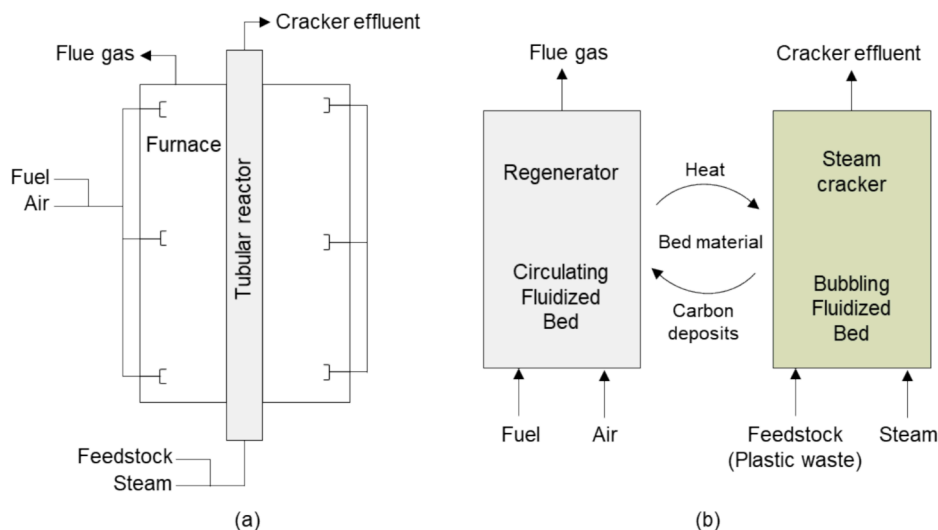
Fig. 4. Schematics of a tube from a conventional steam cracker and a DFB steam cracker.

Table 1
Sampling and analysis techniques applied to each slipstream of the product gas mixture.

	Sampling technique	Species measured	Analytical instrument
Slipstream 1	Product gas scrubbed with isopropanol at −17 °C	He, N_2, O_2, H_2, CO, CO_2, CH_4, C_2H_2, C_2H_4, C_2H_6, C_3H_6, and C_3H_8	GC-TCD: Varian CP4900 micro-GC equipped with Poraplot Q and MS5A columns. Isothermal program: 65 °C (PPQ) and 80 °C (MS5 A).
	Product gas collected in a Tedlar® gas bag	C_3H_4, C_3H_6, C_3H_8, C_4H_4, C_4H_6, C_4H_8, C_5H_6, C_5H_8, C_5H_{10}, C_5H_{12}, C_6H_6, C_6H_{10}, C_6H_{12}, and C_6H_{14} (all isomers measured individually)	GC-VUV: Thermo Scientific TRACE 1310 equipped with CP-Sil5 CB column and VUV Analytics VGA-100 detector. Temperature program: 35 °C (1 min) – 102.5 °C, 30 °C/min.
	Product gas sampled through a series of 2 solid-phase adsorption (SPA) columns.	Benzene, toluene, xylenes, styrene, naphthalene, and other PAHs	GC-FID: BRUKER GC-430 equipped with BR-17-ms column. Temperature program: 50 °C (5 min) – 350 °C, 8 °C/min, final hold 7.5 min.
Slipstream 2	Product gas reacted at 1700 °C in HTR.	He, H_2, CO, and CO_2	GC-TCD: Varian CP4900 micro-GC equipped with Poraplot U and MS5A columns. Isothermal program: 65 °C (PPU) and 80 °C (MS5 A).

regulated by a Bronkhorst® model F-202AV mass flow controller. The concentrations obtained from the GC analyses are converted into product yields using the helium balance and expressed in terms of moles or mass of the product species per unit mass of the feedstock. For a detailed description of the sampling and analytical techniques used in this work, readers may refer to the work performed by Mandviwala et al., which establishes a complete carbon balance over the Chalmers DFB steam cracker [45].

2.4. Bed material

The steam cracker is operated with silica sand as the fluidizing bed material. Table 2 provides the physical properties and chemical composition of the silica sand.

Table 2 presents the properties of the bed material before its introduction into the DFB unit. The physical properties and chemical composition of silica sand undergo gradual changes once introduced into the DFB steam cracker. These transformations include structural modifications due to reductive-oxidative cycles, exposure to high temperatures, and thermal and mechanical stresses. The silica sand also experiences an accumulation of chemical species originating from the ash content of the steam cracker feedstock and the biomass fed into the regenerator. Nevertheless, the properties of the bed material are maintained by replacing approximately 5 % of the bed material in the DFB system with fresh bed material every day.

2.5. Feedstocks

Table 3 provides an overview of the feedstocks, describing their polymer composition and relevant chemical characteristics.

The feedstocks outlined in Table 3 originate from multiple sources. Naphtha and PE stand out as clean feedstocks directly supplied by their producers. Naphtha, provided by Preem AB in Gothenburg, Sweden, is light straight run naphtha primarily composed of aliphatic hydrocarbons from C4 to C8. The PIONA composition of the naphtha, analyzed using the GC-VUV method developed by Dunkle et al. [46], is detailed in Table S1 (supplementary information). The PE pellets were provided by Borealis AB in Stenungsund, Sweden. The chemical composition of the PE pellets, determined by proximate and ultimate analysis, is provided in Table S2 (supplementary information).

Table 2
Physical properties and chemical composition of the fluidizing bed material silica sand.

Physical properties	
Particle density (kg/m^3)	2650
Mean diameter, d_p (μm)	200
Chemical composition (%wt.)	
SiO_2	90
Al_2O_3	5.5
Fe_2O_3	0.6
Na_2O	1.2
K_2O	1.8

Table 3
A brief description of the materials used as feedstocks in the Chalmers DFB steam cracker.

Feedstock	Polymer types	Chemical characteristics	Description
Naphtha		high paraffin content, low aromatic content, low olefin content	Light straight run petroleum naphtha
Polyethylene (PE)	PE	high polyolefin content, low ash content, low oxygen content	Virgin polymer pellets
Mixed packaging waste (MPW)	PE, PP, PET, PVC, PU, PA, PS, Cellulose	medium polyolefin content, high PET & PS content, high ash content	Post-consumer unsorted packaging plastic waste
Cardboard recycling reject (CRR)	PE, PP, PET, PVC, Cellulose	medium polyolefin content, high cellulose content, high ash content	Reject fraction from cardboard recycling. Multilayer films of cellulose and plastics.
Mechanical recycled polyolefins (MRP)	PE, PP	high polyolefin content, low oxygen content, low ash content	Mechanically recycled post-consumer polyolefin mixture
Pyrolysis oil		high aliphatic content, high olefin content, low oxygen content, low ash content	Post-consumer polyolefin pyrolysis oil (non-hydrotreated)

Table 3 also lists different plastic wastes utilized in this study: Mixed packaging Waste (MPW), Cardboard Recycling Reject (CRR), and Mechanically Recycled Polyolefins (MRP). MPW, sourced from domestic packaging waste streams, consists of different polymers, predominantly polyolefins. CRR, obtained as a waste fraction from the cardboard recycling process, is a multi-layered mix of cellulose and polyolefins that resist separation via traditional pulping methods. Additionally, CRR contains some PET and PVC. MRP is composed of mechanically recycled post-consumer PE and PP. Table 4 provides the polymer composition of these waste streams, calculated using a model developed by Forero Franco et al. [47]. This model utilizes the elemental composition and lower heating value to estimate the polymeric composition of the feedstocks. The detailed elemental compositions of these wastes can be found in Table S2 (supplementary information).

The selection of plastic wastes for this work ensures variability in polymer composition while considering the practical availability of these waste streams in real-life scenarios. The variability in the polymer composition centers around the polyolefin content of the feedstock. Additionally, using the waste streams without pretreatment and pre-sorting ensures that the selected waste streams are readily available and suitable for processing in a DFB steam cracker.

Pyrolysis oil was derived from the thermal pyrolysis of post-consumer polyolefins. The producer of the pyrolysis oil is not disclosed due to confidentiality reasons. This pyrolysis oil is characterized by its high olefin content and is used without undergoing pretreatment steps such as hydrotreatment and distillation. The PIONA composition of the pyrolysis oil, determined using the GC-VUV method developed by Dunkle et al. [46], is provided in Table S1 (supplementary information).

2.6. Operational parameters

The operational parameters were varied to explore the performance

Table 4
Polymeric composition of the mixed plastic wastes used in this. Calculated based on the model developed by Forero Franco et al. [47].

Feedstock	PE + PP	Cellulose	PS	PET	PVC	PA
%weight. of dry feedstock						
MPW	45.80	20.90	9.32	10.12	1.30	4.20
CRR	47.50	38.90	<0.01	8.75	0.40	4.44
MRP	100	<0.01	<0.01	<0.01	<0.01	<0.01

and flexibility of the reactor system. These parameters include the feeding rate, temperature in the particle distributor (T1), temperature in the steam cracker (T2), and the bed material circulation rate. The six different feedstocks were subjected to these variations, resulting in a comprehensive experimental matrix consisting of 33 unique operational points, as shown in Table 5. The specific operational parameters corresponding to each unique point are detailed in Tables S3 and S4 (supplementary information).

The feeding rates demonstrate the scalability of the DFB steam cracking process. Although the steam cracker has a feedstock processing capacity of 350 kg/h PE, the experimental matrix was restricted to a maximum feeding rate of 120 kg/h PE. This limitation is due to the extruder, which has a maximum feeding rate of 135 kg/h. Additionally, the research facility's location at the center of a university campus imposed restrictions on storing plastic waste and highly flammable liquids. Consequently, feeding rates for plastic wastes and liquid feedstocks were kept below 50 kg/h to comply with safety and storage regulations.

As previously mentioned, temperature T2 is equivalent to the COT of a conventional steam cracker and is a critical parameter for evaluating the cracking temperature. Conventional steam cracking operates at a COT of 800–850 °C to promote the formation of light olefins. Therefore, the T2 temperature range was selected with a maximum of 825 °C, aiming to enhance light olefin production. The lower end of the T2 range corresponds to the minimum achievable temperature in the Chalmers DFB steam cracker. This wide temperature range was chosen to demonstrate the flexibility of the process.

The range of bed material circulation rate selected in this study covers the entire achievable range in the Chalmers DFB unit. It's important to note that among the four parameters listed in Table 5, only the feeding rate is independent. The other three parameters, temperature in the particle distributor (T1), temperature in the steam cracker (T2), and bed material circulation rate, are interdependent. This interdependency is governed by the heat balance over the DFB.

Each operational point requires approximately three hours, which includes the time needed to reach the desired set points and achieve stable operation. Within this timeframe, each operational point includes at least one hour of stable operation. This duration allows sufficient time for collecting relevant samples from the steam cracker, ensuring comprehensive data collection during steady-state conditions. The results presented in the following section are the average values obtained

Table 5
Operational parameters of the Chalmers DFB steam cracker investigated in this work.

Feedstock	Feeding rate (kg/h)[a]	Temperature, T1 (°C)	Temperature, T2 (°C)	Bed material circulation (kg/m^{2}s)	Number of operational points
Naphtha	40	795–840	750–810	N/A[b]	7
PE	60–120	780–850	700–825	40–90	15
MPW	50	760–850	720–810	60–85	3
CRR	50	785–845	750–800	45–65	2
MRP	50–100	780–815	750–790	55–135	4
Pyrolysis oil	28	760–800	720–760	55	2

[a] Feeding rate (kg/h) calculated on dry basis
[b] Measurement not available

during the stable operation periods.

3. Results

The results are presented as the contribution of individual product species to the carbon balance (% carbon by weight), representing the yield of each species in the product gas relative to the carbon in the feedstock on a dry basis. This method provides a clear understanding of the conversion of carbon atoms from the feedstock into different species in the steam cracker.

It is common practice to report yields as %weight of the feedstock in the field of steam cracking. The results reported as %carbon can be converted to %weight using the carbon content of the feedstock (Table S2, supplementary information) and the molecular weight of the individual species for a fair comparison.

Trends demonstrating the conversion rates and production distributions from all operational points are presented. These trends show the yields of industrially relevant species, including methane, ethylene, propylene, C4 olefins, BTXS, and CO_x. The overall carbon balance involves more than 60 species, with individual yields detailed in Tables S5 to S8 (supplementary information). Fig. 5 summarizes the yields (% carbon) of the industrially relevant species obtained from all operating points with naphtha as the feedstock. This figure highlights the correlation between the yields of different species and cracking temperature.

The results presented in Fig. 5 show notable trends in product yields as the cracking temperature increases from 750 °C to 810 °C. Methane and ethylene yields increase consistently with temperature, reaching nearly their highest values at 800 °C, with methane at 15 % and ethylene at 34 %. Beyond 800 °C, there is no significant increase in the yields of methane and ethylene. Conversely, propylene yield decreases from 17 %

at 750 °C to 11 % at 810 °C, and C4 olefins show a similar trend. These trends suggest that higher cracking temperatures promote the further breakdown of propylene and C4 olefins into smaller molecules such as methane and ethylene.

The yields of BTXS and CO_x also increase with rising cracking temperatures. BTXS yield increases from 5 % at 760 °C to 7 % at 780 °C. Similarly, CO_x yield increases from 5 % to 13 % over the entire temperature range. These trends indicate that higher temperatures favor aromatization reactions and oxidation of the feedstock. The oxidation occurs due to the oxygen transfer phenomenon. As explained earlier, this oxygen transfer phenomenon occurs because of certain oxygen-containing species in the bed material. Some CO_x may also form due to the steam reforming reaction on the surface of the bed material.

A notable similarity exists between the trends observed here and those in conventional steam cracking of naphtha. Researchers have extensively explored the impact of COT on steam cracker yields, focusing on optimizing ethylene and propylene production [48]. In conventional naphtha cracking, methane and ethylene yields typically increase with COT, while the yields of propylene and butenes decrease. According to Gholami et al., ethylene yield peaks at 25 % (by weight) within a COT range of 750–830 °C, with methane reaching approximately 15 % in the same range [2]. Several other studies have demonstrated a maximum ethylene yield of approximately 30 % within a COT range of 800–850 °C. The yields of propylene and butenes in conventional steam cracking generally range from 15 % to 20 % and 8 % to 10 %, respectively. The carbon oxides typically yield around 0.1 % from conventional steam cracking, which is significantly lower than the yields obtained in this work [49–52]. Fig. 6 presents the yields (% weight) obtained in this study and those reported in the literature for conventional steam cracking.
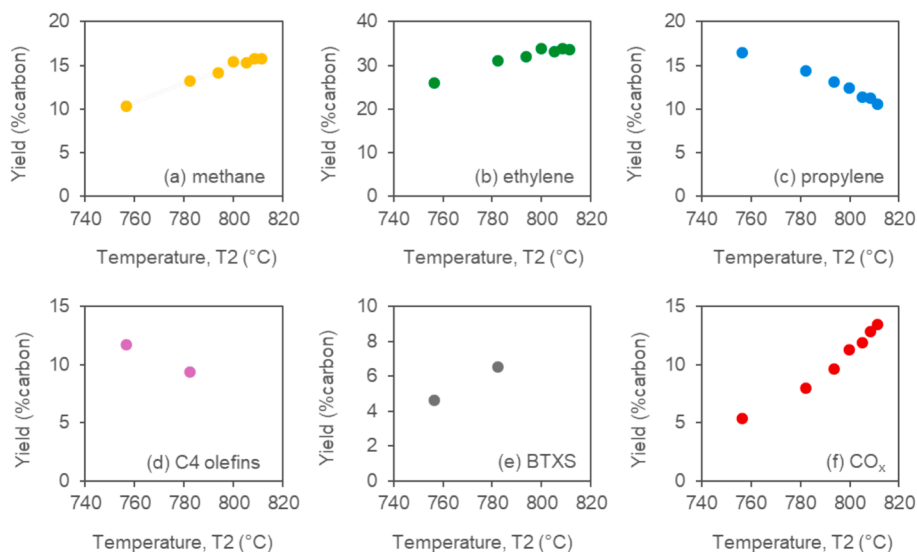

Fig. 5. Yields of (a) methane, (b) ethylene, (c) propylene, (d) C4 olefins, (e) BTXS, and (f) CO_x obtained from steam cracking of naphtha in the Chalmers DFB steam cracker. Temperature T2 (°C) represents the cracking temperature.
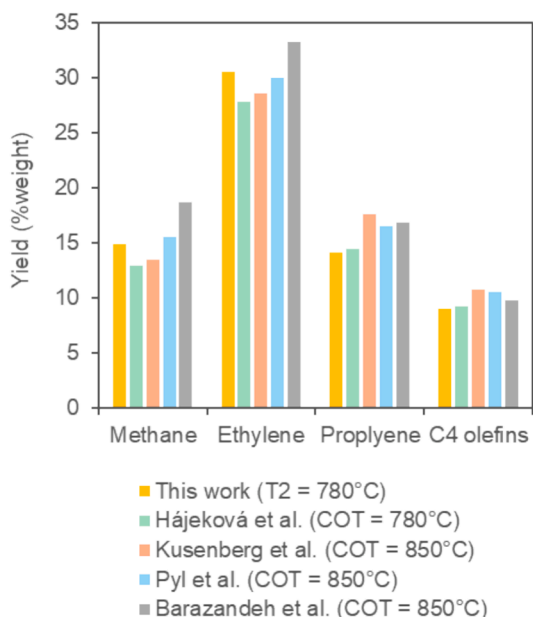
Fig. 6. Comparison of yields (% weight) of methane, ethylene, propylene, and C4 olefins between the Chalmers DFB steam cracker and conventional steam cracking results reported by Hájeková et al., Kusenberg et al., Pyl et al., and Barazandeh et al. [51–54].

Fig. 6 shows that the yields of methane, ethylene, propylene, and C4 olefins are generally similar to those reported for conventional steam crackers by Hájeková et al., Kusenberg et al., Pyl et al., and Barazandeh et al. [49–52]. Minor differences in the yields are because of the variations in the naphtha quality across different studies. However, a significant difference can be observed in the cracking temperature, attributable to the differences in heat transfer properties between fluidized bed and tubular reactors.

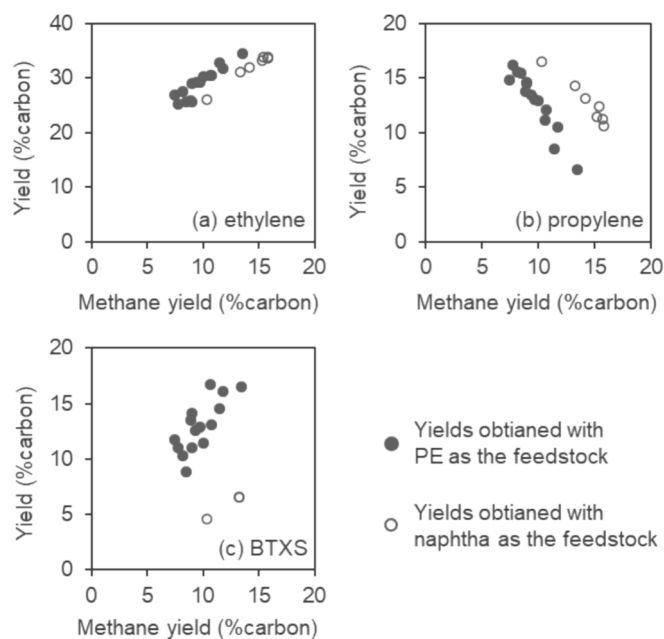It is crucial to note that while Fig. 5 utilizes temperature T2 to illustrate the shift in product distribution, other variations in operating conditions also influence the product yields. The data points in Fig. 5 also encompass variations in bed material circulation rate and feed flow to the steam cracker. Each parameter independently influences the degree to which naphtha is broken down into smaller molecules, generally known as cracking severity.

An alternative to using individual operating parameters is to use methane yield as an indicator of cracking severity, as proposed by Van Geem et al. for conventional steam crackers [48]. The cracking severity and resulting product yields from two or more steam cracking operations can be compared independently of the operating conditions by analyzing the methane yield. Fig. 7 compares the yields of ethylene, propylene, and BTXS obtained with PE and naphtha. Methane yield serves as an indicator of cracking severity in this comparison.

The results presented in Fig. 7 indicate a clear correlation between the yield of methane and the yields of other products, illustrating how the product distribution evolves as the cracking severity increases. The yield of ethylene obtained with PE shows an increasing trend with cracking severity, reaching a maximum of 34 %. Conversely, propylene yield decreases as cracking severity increases, dropping from a maximum of 16 % to a minimum of 7 %. The yield of BTXS also shows a distinct increasing trend with cracking severity, increasing from 9 % to 17 %.

The yields of ethylene, propylene, and BTXS obtained with PE as the feedstock are comparable to those reported in the literature for the thermochemical conversion of PE in fluidized beds. Wilk et al. achieved an ethylene yield of 23 % (by weight) from steam cracking of PE at 850 °C in a DFB [37]. Kaminsky's work reported maximum yields of ethylene at 25 %, propylene at 9 %, and BTXS at 17 % from fluidized bed pyrolysis of PE [53]. Similarly, Jung et al., in a fluidized bed pyrolysis process, obtained maximum yields of ethylene at 22 %, propylene at 10 %, and BTXS at 14 % at a temperature of 730 °C [54].

Fig. 7 also provides a comparative analysis of steam cracking of PE and naphtha. Both feedstocks show notable similarities in the overall trends, particularly in ethylene and propylene yields, which align closely across different cracking severities. However, deviations are evident in methane and BTXS yields. PE shows significantly higher BTXS yields than naphtha, suggesting a stronger tendency for aromatization reactions. In contrast, naphtha yields slightly more methane than PE.

The correlations shown in Fig. 7 suggest that methane yield, the cracking severity index proposed by Van Geem et al. [48], can

Fig. 7. Yields of (a) ethylene, (b) propylene, and (c) BTXS obtained from the Chalmers DFB steam cracker with PE as the feedstock. The yields obtained with naphtha are shown on the same plots for comparing the trends. The yield of methane serves as an indicator of cracking severity.
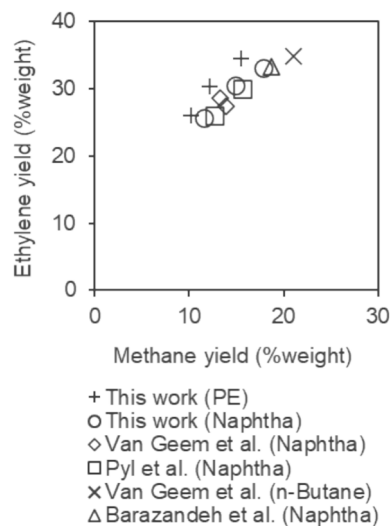

Fig. 8. The ethylene − methane correlation for the yields obtained from the Chalmers DFB steam cracker (this work) and the yields obtained from conventional steam crackers as reported by Van Geem et al. [50], Barazandeh et al. [51], and Pyl et al. [52].
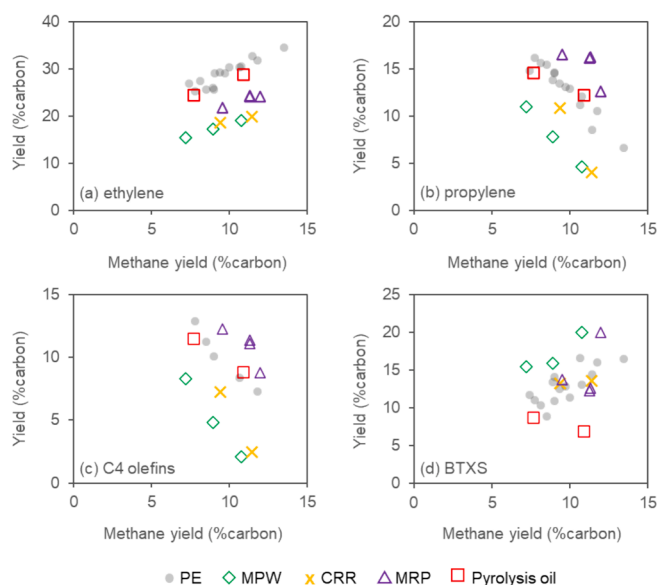
Fig. 9. Yields of (a) ethylene, (b) propylene, (c) C4 olefins, and (d) BTXS obtained from steam cracking of MPW, CRR, MRP, and Pyrolysis oil in the Chalmers DFB steam cracker. The yield of methane serves as the cracking severity index. The yields obtained from steam cracking of PE are shown on the same plots for comparison.

effectively characterize product distributions from a DFB steam cracker. Therefore, this index can describe product distribution independently of the reactor configuration and the feedstock type. To illustrate this, Fig. 8 presents the ethylene-methane correlation for the yields (%weight) obtained in this work and those reported in the conventional steam cracking literature.

Fig. 8 demonstrates that methane yield is a robust cracking severity index, suitable for evaluating steam cracker yields across different reactor configurations. Additionally, this index provides a means to assess product distributions from feedstocks with varying compositions, helping to visualize, for instance, how product yields change with the feedstocks' polymeric compositions. Fig. 9 further illustrates the correlations of light olefins and BTXS with the cracking severity for the other feedstocks used in this work, including MPW, CRR, MRP, and pyrolysis oil.

Fig. 9 also provides the yields obtained with PE as the feedstock, allowing for a comparison with the yields from other feedstocks. Similar trends emerge for all feedstocks across the four correlations shown in Fig. 9. Lower cracking severity favors the production of propylene and C4 olefins while increasing cracking severity results in higher ethylene yields. The total yield of C2 – C4 olefins remains consistent irrespective of the cracking severity for a given feedstock. The yield of BTXS also increases with the increase in cracking severity for most of the data points. Notable deviations become apparent when comparing individual yields with those obtained from PE.

The ethylene yields obtained with pyrolysis oil closely align with those obtained from PE, reaching a maximum of 28 %. In contrast, the ethylene yields for MPW, CRR, and MRP deviate significantly, with all three feedstocks producing less ethylene than PE. Specifically, the ethylene yield for MRP ranges from 22 % to 24 %, while CRR and MPW give ethylene yields ranging from 15 % to 20 %.

Interestingly, pyrolysis oil also yields similar amounts of propylene and C4 olefins compared to PE. Fig. 9 (b) and (c) clearly show that the data points for pyrolysis oil overlap with those for PE. The yields of propylene and C4 olefins for pyrolysis oil range from 12 % to 15 % and 8 % to 12 %, respectively. In contrast, the yields from the other feedstocks, MPW, CRR, and MRP, deviate notably from those of PE. MRP produces slightly higher yields, while CRR and MPW yield significantly lower

amounts of propylene and C4 olefins than PE.

The yields of BTXS obtained with CRR and MRP closely align with those obtained with PE across all the data points. Pyrolysis oil yields the lowest amount of BTXS among the feedstocks, between 7 to 9 %. MPW stands as the only feedstock that shows increased BTXS formation compared to PE, producing yields in the range of 15–20 %.

The deviations observed in Fig. 9 arise from variations in the composition and molecular structures of the feedstocks. Notably, pyrolysis oil and MRP exhibit the closest resemblance to the molecular structure of PE. The pyrolysis oil utilized in this study was derived from the pyrolysis of polyolefins and is, therefore, primarily composed of aliphatic hydrocarbons. Similarly, MRP, which results from the mechanical recycling of well-sorted polyolefins, consists predominantly of PE and PP. As a consequence of their similar chemical compositions to PE, both pyrolysis oil and MRP yield a comparable product distribution to that obtained from PE in terms of light olefin and BTXS production.

In contrast, MPW and CRR contain significantly lower polyolefins than PE and MRP, comprising less than 50 % polyolefins alongside materials like PET, PS, and cellulose. This lower polyolefin content reduces the yield of light olefins, as observed in Fig. 9 for MPW and CRR. To gain a better insight into how polyolefin content affects light olefin production, Fig. 10 illustrates this relationship by plotting the combined yield of ethylene, propylene, and C4 olefins against the polyolefin content of the feedstock.

Fig. 10 also includes the average light olefin yield obtained across all operational points with PE as the feedstock, indicated by a dashed line at 52 %. Points on this dashed line signify that the light olefin yield corresponds to 52 % of the polyolefin content, consistent with PE. For MPW and CRR, the data points closely align with this dashed line, indicating that these feedstocks convert into light olefins in a proportion similar to PE. Moreover, these points lie slightly above the dashed line, suggesting a slightly higher light olefin yield than PE, possibly due to ethylene formation from other polymers like PET and cellulose in these feedstocks. Similarly, data points for MRP also cluster around the dashed line, indicating a selective light olefin production of approximately 52 %.

The non-polyolefin components in MPW and CRR, such as PET, PS, and cellulose, are characterized by their molecular structures containing aromatic rings and oxygen atoms. During steam cracking, these feedstocks are expected to favor the production of aromatic hydrocarbons and carbon oxides due to these structural features. Fig. 9(d) illustrates the increased formation of BTXS for MPW, attributable to the significant
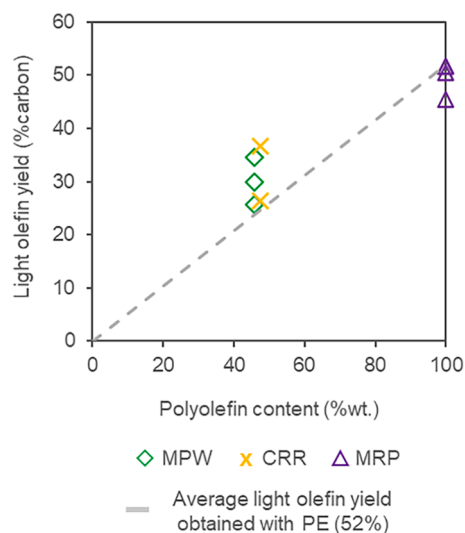

Fig. 10. Correlation between the light olefin (C2 – C4) yield and the polyolefin content of the feedstock. The dashed line signifies the average light olefin yield obtained with PE (100 % polyolefin).
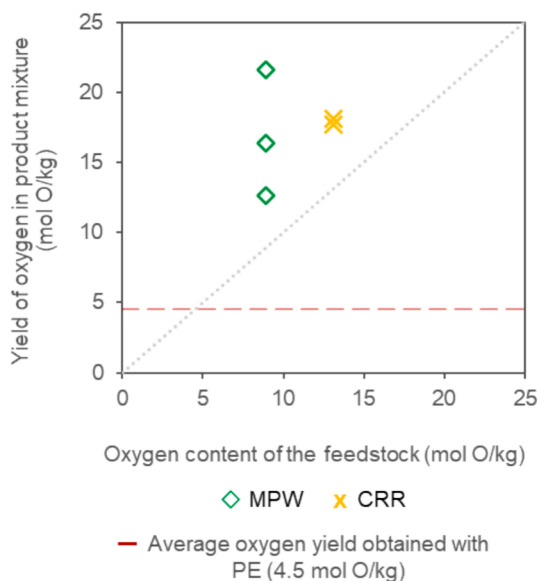
9

Fig. 11. Correlation between the yield of oxygen obtained from the Chalmers DFB steam cracker and the oxygen content of the feedstock. The horizontal dashed line on the plot shows the average oxygen yield obtained with PE and provides a reference. The diagonal dashed line on the plot corresponds to an equal amount of oxygen in the product gas and the feedstock.

presence of PET and PS in this feedstock. Conversely, CRR resembles PE in BTXS yield due to CRR's non-polyolefin content, which is predominantly cellulose, a non-aromatic polymer.

The presence of oxygen atoms in the molecular structures of PET and cellulose is reflected in the oxygen content of the feedstocks (see Table S2, supplementary information). It is implied that the oxygen content of the feedstock will result in oxygen in the product mixture. Fig. 11 illustrates this correlation between the yield of oxygen atoms in the product mixture and the oxygen content of the feedstock.

Fig. 11 shows the yield of oxygen (mol/kg of dry feedstock) in the product mixture for MPW and CRR. It is important to note that the oxygen yield corresponds exclusively to carbon oxides. The oxygen yield in the form of hydrocarbons is negligible and disregarded in this plot. The red dashed line in the figure represents the average oxygen yield obtained with PE as the feedstock, which is 4.5 mol/kg. Another dashed line passing through the origin indicates an equivalent amount of oxygen in the feedstock and the product mixture. Notably, all data points for MPW and CRR fall above this dashed line, showing higher oxygen amounts in the product mixture than in the feedstock. As discussed earlier, the excess oxygen in the product mixture likely arises due to the oxygen transport phenomenon that induces an oxidizing environment in the steam cracker. The steam reforming of hydrocarbons or the water gas shift reaction may also contribute to the formation of carbon oxides.

Fig. 11 clearly shows that the yield of carbon oxides is significant for feedstocks containing cellulose and PET. The data points obtained with PE and naphtha also indicate notable carbon oxide formation compared to a conventional steam cracker. The increased production of carbon oxides underscores the need for effective conversion of these carbon oxides into molecular building blocks to achieve complete recyclability of the feedstock.

The carbon oxides, methane, and hydrogen derived from a DFB steam cracker offer the potential for conversion into molecular building blocks through synthesis processes like MTO and FT. These processes typically require an R ratio of 2 for optimal conversion [55]. Fig. 12 presents the average R ratio of the CH_4, CO_x, and H_2 mixture obtained from all the feedstocks presented in this work.

Fig. 12 shows a clear distinction in R ratios between oxygen-containing feedstocks and those without oxygen content. Feedstocks
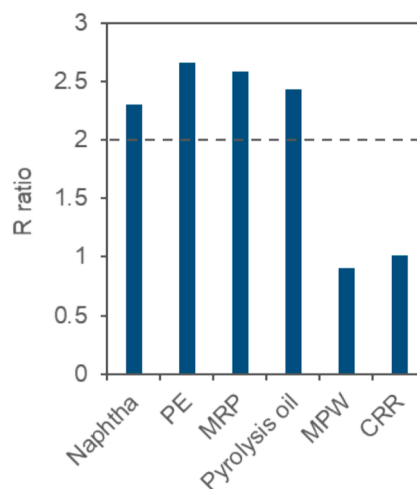

Fig. 12. The R ratio of the CO, CO_2, CH_4, and H_2 mixture obtained from the Chalmers DFB steam cracker. The R ratios presented here are average values obtained with each investigated feedstock. The R ratio is defined as R = (H_2 − CO_2)/(CO + CO_2).
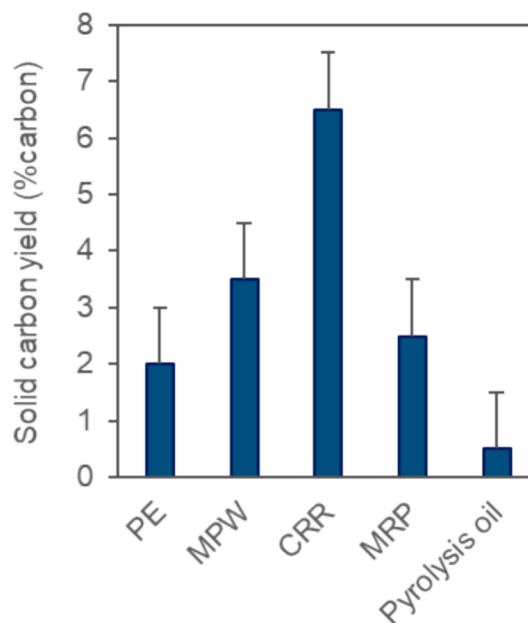

Fig. 13. The yield of solid carbon obtained from the Chalmers DFB steam cracker. The values represent the average yield obtained with each investigated feedstock. The error bars represent the approximate amount of solid carbon overestimated due to coke formation in the HTR.

such as naphtha, PE, MRP, and pyrolysis oil, which do not contain oxygen (see Table S2, supplementary material), consistently yield R ratios above 2. In contrast, MPW and CRR, which contain oxygenated polymers, have significantly lower R ratios. The lower R ratios obtained with oxygen-containing feedstocks indicate an additional requirement for hydrogen in downstream synthesis processes to achieve complete conversion of syngas into molecular building blocks.

The formation of solid carbon during steam cracking is also assessed. As discussed earlier, the amount of solid carbon is estimated using the HTR method developed by Israelsson et al. [44]. Fig. 13 presents the average yield of solid carbon obtained from PE, MPW, CRR, MRP, and pyrolysis oil across all the operational points. The amount of solid carbon formed in HTR is approximately 1 % (% carbon), which causes an overestimation of the solid carbon formed in the steam cracker. This

overestimation is indicated by the error bars in Fig. 13.

Fig. 13 illustrates significant variations in carbon deposition depending on the feedstock used. Pyrolysis oil exhibits the lowest yield of solid carbon at 0.5 %. Pure polyolefin feedstocks like PE and MRP show solid carbon yields of 2 % and 2.5 %, respectively. MPW demonstrates a slightly higher yield of solid carbon than the pure polyolefin feedstocks, averaging 3.5 %. CRR stands out with the highest solid carbon yield among the feedstocks examined, reaching 6.5 %. The variations in the yield of solid carbon are attributable to differences in the polymeric composition of the feedstocks. Pyrolysis oil, PE, and MRP, which are predominantly aliphatic, exhibit lower susceptibility to carbonization reactions. In contrast, CRR and MPW contain significant amounts of cellulose and PET, leading to char formation during steam cracking.

The formation of solid carbon is analogous to coke formation in conventional steam crackers. A conventional naphtha cracker yields approximately 0.01 % coke (% weight). However, when conventional steam crackers incorporate polyolefin pyrolysis oils, the coke yield escalates significantly, often by two to tenfold [52]. The increased production of coke substantially impacts the economic viability of a conventional steam cracker due to the necessity for frequent decoking procedures.

The yield of carbon deposits from the Chalmers DFB steam cracker underscores its capability to operate continuously without intermittent decoking procedures. Even in cases such as CRR, which shows significantly higher solid carbon formation than conventional steam crackers, no operational difficulties were observed throughout the experimental campaign. That is attributable to the continuous removal of carbon deposits with the bed material.

The results in Figs. 5 through 13 highlight the trends and yields (% carbon) of key product species obtained in this study. These trends provide a comprehensive understanding of how the product distribution from a DFB steam cracker evolves under various operating conditions and with different feedstocks, including pure polyolefins and unsorted plastic waste fractions. To further enhance this understanding, Table 6 shows the absolute yields (kg/kg of dry feedstock) of the product species obtained under one specific operating condition for each of the six different feedstocks used in the study. The yields reported in Table 6 are derived by converting the % carbon yields presented in Tables S5 to S8 (Supplementary information).

Table 6 compares the absolute yields obtained with the six feedstocks under similar operating conditions. Additionally, the absolute yield values can be directly compared to yields reported in the literature on thermochemical recycling of plastics and those obtained from industrial steam cracking processes. Although Table 6 excludes products with yields below 0.01 kg/kg, such as cis/trans-2-butene, propadiene, xylenes, and a few others, the yields of these species are in the Supplementary Information.

4. Discussion

The results support the hypothesis that steam cracking in a DFB reactor configuration is fundamentally equivalent to the conventional steam cracking process. The yield of methane, proposed as a cracking severity index for conventional steam crackers, effectively characterizes the product distributions from the Chalmers DFB steam cracker. The correlations between product yields and the cracking severity index offer experimental validation of the steam cracking mechanism reported in the literature [48], demonstrating their applicability to large-scale DFB steam crackers. As the cracking severity increases, the product distribution becomes enriched with light hydrocarbons and monoaromatics. Notably, the correlation between methane yield and temperature illustrates the applicability of the chain-end scission reaction. Furthermore, higher cracking temperatures lead to increased yields of ethylene and monoaromatics because of enhanced secondary reactions, such as beta-scission and cyclization. These correlations indicate that the cracking severity achieved in a DFB steam cracker within the temperature range of 700–825 °C is suitable for the selective production of light olefins and monoaromatics, which can constitute up to 65 % (% carbon) of the product mixture.

The results also demonstrate the capability of a DFB steam cracker to break down hydrocarbons with longer aliphatic chains than naphtha, a capability that conventional steam crackers do not possess. The DFB steam cracker shows selective production of light olefins and BTXS, achieving a combined 52 % yield of ethylene, propylene, and C4 olefins, along with a 15 % yield of BTXS from a pure polyolefin feedstock. These findings provide experimental proof that one-step selective production of light olefins and monoaromatics from polyolefins is achievable in a DFB steam cracker without the use of any catalyst.

The findings outlined in this work also underscore the potential of leveraging a DFB steam cracking process to process unsorted plastic wastes. Despite variations in polymer composition, the DFB steam

Table 6

Absolute yields (kg/kg of dry feedstock) of products for each of the six feedstocks under a selected operating condition of the Chalmers DFB steam cracker. Products with yields below 0.01 kg/kg are excluded.

	Naphtha	PE	MPW	CRR	MRP	Pyrolysis oil
Temperature, T2 (°C)	782	783	768	742	789	755
Feeding rate (kg/h)	40	90	50	50	100	28
Yield (kg/kg$_{dry-feedstock}$)						
Hydrogen	0.0160	0.0110	0.0110	0.0120	0.0100	0.0100
Carbon monoxide	0.0450	0.0170	0.0640	0.1070	0.0210	0.0300
Carbon dioxide	0.1760	0.0800	0.3100	0.3060	0.0660	0.0850
Methane	0.1490	0.1220	0.0790	0.0750	0.1370	0.1240
Ethylene	0.3050	0.3040	0.1340	0.1310	0.2420	0.2880
Ethane	0.0200	0.0370	0.0180	0.0200	0.0600	0.0270
Propylene	0.1410	0.1120	0.0610	0.0760	0.1260	0.1230
Propane	0.0080	0.0080	0.0040	0.0130	0.0080	0.0080
1,3-butadiene	0.0460	0.0640	0.0250	0.0360	0.0470	0.0530
1-butene	0.0106	0.0132	0.0011	0.0000	0.0065	0.0184
Isobutylene	0.0191	0.0005	0.0078	0.0104	0.0198	0.0107
C5 olefins	0.0230	0.0157	0.0050	0.0060	0.0200	0.0130
Benzene	0.0490	0.1040	0.0680	0.0550	0.1150	0.0390
Toluene	0.0070	0.0320	0.0210	0.0170	0.0440	0.0160
Styrene	0.0040	0.0160	0.0250	0.0120	0.0210	0.0080
PAHs	0.0070	0.0340	0.0270	0.0180	0.0420	0.0160
Solid carbon	<0.005	0.0236	0.0231[a]	0.0394	0.0262	<0.005

[a] Yield corresponds to the operational point with T2 = 721 °C.

cracker selectively produces light olefins from unsorted plastic waste streams. The conversion of the polyolefin content of the waste stream into light olefins occurs in a proportion similar to that of PE, approximately 52 %. Importantly, this proportion remains consistent regardless of the presence of other polymers in the waste.

The non-polyolefin content of plastic waste streams in society is predominantly PET, PS, and cellulose. While these non-polyolefin materials are also effectively converted in the DFB steam cracker, they yield less valuable products than light olefins. The presence of non-polyolefin content in the feedstock is reflected in the increased yield of aromatics and carbon oxides in the product mixture. That is because aromatic and oxygenated polymer structures of non-polyolefins effectively break down into aromatics and carbon oxides within the DFB steam cracker. It highlights the DFB steam cracker's ability to differentiate between polyolefin and non-polyolefin contents of plastic waste during conversion. Separating the cracking products in the downstream gas separation units provides in-situ sorting capabilities to the overall process. However, since the downstream gas separation is energy-intensive, one must make a trade-off between presorting the feedstock and separating the cracking products.

Steam cracking in a DFB offers another significant advantage over tubular reactors by handling feedstocks prone to coke formation, such as pyrolysis oils. The results indicate that feedstocks containing PET and cellulose are also susceptible to coke formation. However, the robust design of the DFB reactor configuration enables the continuous removal of solid carbon deposits, facilitating uninterrupted steam cracking operations. This capability of the DFB steam cracking process makes it well-suited for processing non-hydrotreated pyrolysis oils derived from mixed plastic wastes. These findings present an opportunity for the existing petrochemical clusters to transform into thermochemical recycling plants by replacing conventional steam crackers with DFB steam crackers. However, it is crucial to note that DFB steam crackers cannot replace conventional ethane crackers since ethane crackers are specialized units and have limited product gas separation capabilities.

The gas separation units downstream of conventional naphtha crackers do not require replacement, as the product distributions from both steam crackers are similar. However, additional gas treatment steps may be necessary downstream of DFB steam crackers before introducing the product gas into the existing gas separation units. The current gas separation units cannot handle high concentrations of carbon oxides because conventional steam cracking units yield only marginal amounts of carbon oxides, typically less than 0.1 %. In contrast, DFB steam crackers will likely produce significant amounts of carbon oxides due to the oxygen content of mixed plastic wastes and the inherent reactions occurring within the steam cracker. A DFB steam cracker must have a downstream water gas shift reactor and an acid gas removal unit to manage the carbon oxides.

Guard beds and adsorbents downstream of a DFB steam cracker may also be necessary to remove species that could poison downstream catalytic processes, such as polymerization or hydrogenation. Some of the known poisons to Ziegler-Natta polymerization catalysts include methyl mercaptan (CH_4S), carbon disulfide (CS_2), and methyl cyanide (CH_3CN) [56]. While this work does not investigate the formation of these species during the steam cracking of plastic waste, this remains an open topic for further research.

As an introductory exploration of steam cracking in DFB, this work opens opportunities for further research towards the applicability and economic viability of the process. Future research should focus on several key areas to strengthen the applicability of such a steam cracking process. Since steam cracking reactions are kinetically driven, the influence of heat transfer rates on the kinetics and residence time requires thorough investigation. Understanding how heat transfer affects these factors is crucial for optimizing the light olefin yield from a DFB steam cracking process. Additionally, the fluidization regimes and the behavior of solid plastic particles in DFB steam crackers need dedicated investigations. Insights into these areas will help improve the overall

heat transfer rates achieved in a DFB steam cracker.

Conventional naphtha crackers are energy-independent and use an integrated heat exchanger network to recover heat from the cracker effluent [3]. This recovered heat preheats the feedstock and generates steam, minimizing external energy input. The steam cracking of PE is estimated to have an endothermic reaction heat of 2.0–2.5 MJ/kg based on the results obtained in this work. The overall energy requirement will be slightly higher, considering the additional energy needed to heat the feedstock and steam to reaction temperatures. While this study does not focus on the energy balance over a DFB steam cracker, further research is essential. In particular, developing integrated heat recovery systems for solid feedstocks could significantly enhance the energy efficiency of the process.

The pyrolysis oil used in this study was derived from the pyrolysis of well-sorted polyolefins. Future research should investigate the steam cracking of pyrolysis oils obtained from unsorted plastic wastes. That would necessitate directing pyrolysis research toward producing oils from mixed plastic wastes. Additionally, efforts towards minimizing the production of off-gases during the pyrolysis process will be beneficial. These initiatives are crucial for improving the circularity and sustainability of the pyrolysis process.

Pyrolysis stands out as a highly versatile thermochemical recycling process. However, the efforts in the hydrotreatment of pyrolysis oil significantly influence its economic viability. In addition, pre-sorting the plastic waste to obtain naphtha-like pyrolysis oil further impacts the economics of the process. Introducing a DFB steam cracker could revolutionize this landscape by eliminating the need for pre-sorting and hydrotreatment. Pyrolysis oils from mixed plastic wastes could serve as drop-in feedstocks for the DFB steam cracking process, potentially enhancing the economic feasibility of pyrolysis as a sustainable thermochemical recycling solution.

5. Conclusions

This work demonstrates that steam cracking in a DFB reactor is equivalent to steam cracking in tubular reactors. The cracking mechanisms and severity indices applicable to conventional steam crackers also apply to DFB steam crackers. The cracking severity achieved within the temperature range of 700–825 °C in a DFB steam cracker is suitable for the selective production of light olefins and monoaromatics.

Steam cracking of pure polyolefin feedstocks in DFB results in an average yield (%carbon) of 52 % light olefins and 15 % BTXS. When processing plastic wastes, the conversion of the polyolefin content into light olefins remains consistent at approximately 52 %, regardless of the presence of other polymers. Common non-polyolefin materials in plastic waste, such as PET, PS, and cellulose, are selectively converted into aromatics and syngas. This selective conversion of polyolefin and non-polyolefin contents in a DFB steam cracker provides an in-situ sorting mechanism, eliminating the need for pre-sorting plastic waste.

Coke formation in a DFB steam cracker remains as significant as in conventional steam crackers, particularly for feedstocks with PET and cellulose. However, the DFB steam cracker's ability to continuously remove carbon deposits eliminates the need for intermittent decoking procedures. This capability also facilitates the steam cracking of olefin-rich pyrolysis oils, which are prone to coke formation. When steam cracking a polyolefin pyrolysis oil in DFB, the yield of light olefins is similar to that obtained with pure polyolefin feedstocks despite the high olefin content. These findings demonstrate that a DFB steam cracker eliminates pretreatment steps like distillation and hydrotreatment, essential for processing pyrolysis oils in conventional steam crackers. These results also encourage plastic pyrolysis researchers to widen the scope of feedstocks to unsorted plastic wastes for their pyrolysis processes.

Overall, this work highlights the potential of DFB steam crackers in the thermochemical recycling of plastic waste. Future research should investigate the formation of species that may poison downstream

polymerization processes. Investigations into additional gas separation units required to remove such undesirable species from the product gas are also essential. These efforts will ensure a seamless transition from conventional steam crackers to DFB steam crackers.

6. Funding sources

CRediT authorship contribution statement

Chahat Mandviwala: Writing – original draft, Methodology, Investigation, Data curation, Conceptualization. **Renesteban Forero Franco:** Methodology, Investigation, Data curation, Conceptualization. **Teresa Berdugo Vilches:** Writing – review & editing, Supervision, Investigation, Conceptualization. **Ivan Gogolev:** Methodology, Investigation. **Judith González-Arias:** Methodology, Investigation. **Isabel Cañete Vela:** Methodology, Investigation, Conceptualization. **Henrik Thunman:** Writing – review & editing, Supervision, Funding acquisition, Conceptualization. **Martin Seemann:** Writing – review & editing, Supervision, Project administration, Conceptualization.

Declaration of competing interest

The authors declare that they have no known competing financial interests or personal relationships that could have appeared to influence the work reported in this paper.

Acknowledgments

Appendix A. Supplementary material

Supplementary data to this article can be found online at https://doi.org/10.1016/j.cej.2024.156892.

Data availability

No data was used for the research described in the article.

References

[1] B. Young, T.R. Hawkins, C. Chiquelin, P. Sun, U.R. Gracida-Alvarez, A. Elgowainy, Environmental life cycle assessment of olefins and by-product hydrogen from steam cracking of natural gas liquids, naphtha, and gas oil, J. Clean. Prod. 359 (2022), https://doi.org/10.1016/j.jclepro.2022.131884.

[2] Z. Gholami, F. Gholami, Z. Tišler, M. Vakili, A review on the production of light olefins using steam cracking of hydrocarbons, Energies (basel) 14 (2021), https://doi.org/10.3390/en14238190.

[3] T. Ren, M. Patel, K. Blok, Olefins from conventional and heavy feedstocks: Energy use in steam cracking and alternative processes, Energy 31 (2006), https://doi.org/10.1016/j.energy.2005.04.001.

[4] M.A. Alabdullah, A.R. Gomez, J. Vittenet, A. Bendjeriou-Sedjerari, W. Xu, I. A. Abba, J. Gascon, A viewpoint on the refinery of the future: catalyst and process challenges, ACS Catal. 10 (2020), https://doi.org/10.1021/acscatal.0c02209.

[5] Chemistry of Petrochemical Processes, 2001. https://doi.org/10.1016/b978-0-88415-315-3.x5000-7.

[6] I. Cañete Vela, T. Berdugo Vilches, G. Berndes, F. Johnsson, H. Thunman, Co-recycling of natural and synthetic carbon materials for a sustainable circular economy, J. Clean Prod. 365 (2022), https://doi.org/10.1016/j.jclepro.2022.132674.

[7] H. Thunman, T. Berdugo Vilches, M. Seemann, J. Maric, I.C. Vela, S. Pissot, H.N. T. Nguyen, Circular use of plastics-transformation of existing petrochemical clusters into thermochemical recycling plants with 100% plastics recovery, Sustain. Mater. Technol. 22 (2019), https://doi.org/10.1016/j.susmat.2019.e00124.

[8] R. Geyer, J.R. Jambeck, K.L. Law, Production, use, and fate of all plastics ever made, Sci. Adv. 3 (2017), https://doi.org/10.1126/sciadv.1700782.

[9] G. Kwon, D.W. Cho, J. Park, A. Bhatnagar, H. Song, A review of plastic pollution and their treatment technology: A circular economy platform by thermochemical pathway, Chem. Eng. J. 464 (2023), https://doi.org/10.1016/j.cej.2023.142771.

[10] X. Zhao, M. Korey, K. Li, K. Copenhaver, H. Tekinalp, S. Celik, K. Kalaitzidou, R. Ruan, A.J. Ragauskas, S. Ozcan, Plastic waste upcycling toward a circular economy, Chem. Eng. J. 428 (2022), https://doi.org/10.1016/j.cej.2021.131928.

[11] M.S. Abbas-Abadi, Y. Ureel, A. Eschenbacher, F.H. Vermeire, R.J. Varghese, J. Oenema, G.D. Stefanidis, K.M. Van Geem, Challenges and opportunities of light olefin production via thermal and catalytic pyrolysis of end-of-life polyolefins: Towards full recyclability, Prog. Energy Combust. Sci. 96 (2023), https://doi.org/10.1016/j.pecs.2022.101046.

[12] S.D. Anuar Sharuddin, F. Abnisa, W.M.A. Wan Daud, M.K. Aroua, A review on pyrolysis of plastic wastes, Energy Convers. Manag. 115 (2016), https://doi.org/10.1016/j.enconman.2016.02.037.

[13] M. Kutz, Applied Plastics Engineering Handbook: Processing, Materials, and Applications: Second Edition, 2016.

[14] A. López, I. de Marco, B.M. Caballero, M.F. Laresgoiti, A. Adrados, Influence of time and temperature on pyrolysis of plastic wastes in a semi-batch reactor, Chem. Eng. J. 173 (2011), https://doi.org/10.1016/j.cej.2011.07.037.

[15] I.M. Maafa, Pyrolysis of polystyrene waste: A review, Polymers (basel) 13 (2021), https://doi.org/10.3390/polym13020225.

[16] J.F. Mastral, C. Berrueco, J. Ceamanos, Modelling of the pyrolysis of high density polyethylene. Product distribution in a fluidized bed reactor, J. Anal. Appl. Pyrol. 79 (2007), https://doi.org/10.1016/j.jaap.2006.10.018.

[17] M.S. Abbas-Abadi, A. Zayoud, M. Kusenberg, M. Roosen, F. Vermeire, P. Yazdani, J. Van Waeyenberg, A. Eschenbacher, F.J.A. Hernandez, M. Kuzmanović, H. Dao Thi, U. Kresovic, B. Sels, P. Van Puyvelde, S. De Meester, M. Saeys, K.m. Van Geem, Thermochemical recycling of end-of-life and virgin HDPE: A pilot-scale study, J. Anal. Appl. Pyrolysis 166 (2022), https://doi.org/10.1016/j.jaap.2022.105614.

[18] M. Kusenberg, M. Roosen, A. Doktor, L. Casado, A. Jamil Abdulrahman, B. Parvizi, A. Eschenbacher, E. Biadi, N. Laudou, D. Jänsch, S. De Meester, K.m. Van Geem, Contaminant removal from plastic waste pyrolysis oil via depth filtration and the impact on chemical recycling: A simple solution with significant impact, Chem. Eng. J. 473 (2023), https://doi.org/10.1016/j.cej.2023.145259.

[19] S.E. Levine, L.J. Broadbelt, Detailed mechanistic modeling of high-density polyethylene pyrolysis: Low molecular weight product evolution, Polym. Degrad. Stab. 94 (2009), https://doi.org/10.1016/j.polymdegradstab.2009.01.031.

[20] M. Kusenberg, A. Zayoud, M. Roosen, H.D. Thi, M.S. Abbas-Abadi, A. Eschenbacher, U. Kresovic, S. De Meester, K.M. Van Geem, A comprehensive experimental investigation of plastic waste pyrolysis oil quality and its dependence on the plastic waste composition, Fuel Process. Technol. 227 (2022), https://doi.org/10.1016/j.fuproc.2021.107090.

[21] M.S. Abbas-Abadi, M. Kusenberg, A. Zayoud, M. Roosen, F. Vermeire, S. Madanikashani, M. Kuzmanović, B. Parvizi, U. Kresovic, S. De Meester, K.M. Van Geem, Thermal pyrolysis of waste versus virgin polyolefin feedstocks: The role of pressure, temperature and waste composition, Waste Manag. 165 (2023), https://doi.org/10.1016/j.wasman.2023.04.029.

[22] M. Kusenberg, A. Eschenbacher, M.R. Djokic, A. Zayoud, K. Ragaert, S. De Meester, K.M. Van Geem, Opportunities and challenges for the application of post-consumer plastic waste pyrolysis oils as steam cracker feedstocks: To decontaminate or not to decontaminate? Waste Manag. 138 (2022) https://doi.org/10.1016/j.wasman.2021.11.009.

[23] L. Deng, W. Guo, H.H. Ngo, X. Zhang, D. Wei, Q. Wei, S. Deng, Novel catalysts in catalytic upcycling of common polymer wastes, Chem. Eng. J. 471 (2023), https://doi.org/10.1016/j.cej.2023.144350.

[24] E. Selvam, P.A. Kots, B. Hernandez, A. Malhotra, W. Chen, J.M. Catala-Civera, J. Santamaria, M. Ierapetritou, D.G. Vlachos, Plastic waste upgrade to olefins via mild slurry microwave pyrolysis over solid acids, Chem. Eng. J. 454 (2023), https://doi.org/10.1016/j.cej.2022.140332.

[25] X. Chen, L. Cheng, J. Gu, H. Yuan, Y. Chen, Chemical recycling of plastic wastes via homogeneous catalysis: A review, Chem. Eng. J. 479 (2024), https://doi.org/10.1016/j.cej.2023.147853.

[26] A. Eschenbacher, R.J. Varghese, M.S. Abbas-Abadi, K.M. Van Geem, Maximizing light olefins and aromatics as high value base chemicals via single step catalytic conversion of plastic waste, Chem. Eng. J. 428 (2022), https://doi.org/10.1016/j.cej.2021.132087.

[27] R. Palos, E. Rodríguez, A. Gutiérrez, J. Bilbao, J.M. Arandes, Cracking of plastic pyrolysis oil over FCC equilibrium catalysts to produce fuels: Kinetic modeling, Fuel 316 (2022), https://doi.org/10.1016/j.fuel.2022.123341.

[28] H.S. Cerqueira, G. Caeiro, L. Costa, F. Ramôa Ribeiro, Deactivation of FCC catalysts, J. Mol. Catal. A Chem. 292 (2008), https://doi.org/10.1016/j.molcata.2008.06.014.

[29] I. Vollmer, M.J.F. Jenks, R. Mayorga González, F. Meirer, B.M. Weckhuysen, Plastic waste conversion over a refinery waste catalyst, Angew. Chem. – Int. Ed. 60 (2021), https://doi.org/10.1002/anie.202104110.

[30] R. Saab, K. Polychronopoulou, L. Zheng, S. Kumar, A. Schiffer, Synthesis and performance evaluation of hydrocracking catalysts: A review, J. Ind. Eng. Chem. 89 (2020), https://doi.org/10.1016/j.jiec.2020.06.022.

[31] U. Arena, Process and technological aspects of municipal solid waste gasification. A review, Waste Manag. 32 (2012), https://doi.org/10.1016/j.wasman.2011.09.025.

[32] S. Madanikashani, L.A. Vandewalle, S. De Meester, J. De Wilde, K.M. Van Geem, Multi-scale modeling of plastic waste gasification: opportunities and challenges, Materials 15 (2022), https://doi.org/10.3390/ma15124215.

[33] K.I. Dement'Ev, A.D. Sagaradze, P.S. Kuznetsov, T.A. Palankoev, A.L. Maximov, Selective production of light olefins from Fischer-Tropsch synthetic oil by catalytic cracking, Ind. Eng. Chem. Res. 59 (2020), https://doi.org/10.1021/acs.iecr.0c02753.

[34] T. Cordero-Lanzac, A.G. Gayubo, A.T. Aguayo, J. Bilbao, The MTO and DTO processes as greener alternatives to produce olefins: A review of kinetic models and reactor design, Chem. Eng. J. 494 (2024), https://doi.org/10.1016/j.cej.2024.152906.

[35] G. Lopez, M. Artetxe, M. Amutio, J. Alvarez, J. Bilbao, M. Olazar, Recent advances in the gasification of waste plastics. A critical overview, Renew. Sustain. Energy Rev. 82 (2018), https://doi.org/10.1016/j.rser.2017.09.032.

[36] I. Cañete Vela, J. Maric, J. González-Arias, M. Seemann, Feedstock recycling of cable plastic residue via steam cracking on an industrial-scale fluidized bed, Fuel 355 (2024), https://doi.org/10.1016/j.fuel.2023.129518.

[37] V. Wilk, H. Hofbauer, Conversion of mixed plastic wastes in a dual fluidized bed steam gasifier, Fuel 107 (2013), https://doi.org/10.1016/j.fuel.2013.01.068.

[38] A. Larsson, M. Seemann, D. Neves, H. Thunman, Evaluation of performance of industrial-scale dual fluidized bed gasifiers using the chalmers 2–4-MWth gasifier, Energy Fuel 27 (2013), https://doi.org/10.1021/ef400981j.

[39] A. Larsson, H. Thunman, H. Ström, S. Sasic, Experimental and numerical investigation of the dynamics of loop seals in a large-scale DFB system under hot conditions, AIChE J. 61 (2015), https://doi.org/10.1002/aic.14887.

[40] S.S. Chadwick, Ullmann's encyclopedia of industrial chemistry, Ref. Serv. Rev. 16 (1988), https://doi.org/10.1108/eb049034.

[41] T. Berdugo Vilches, H. Thunman, Experimental investigation of volatiles-bed contact in a 2–4 MWth bubbling bed reactor of a dual fluidized bed gasifier, Energy Fuel 29 (2015), https://doi.org/10.1021/acs.energyfuels.5b01303.

[42] S. Pissot, R. Faust, P. Aonsamang, T. Berdugo Vilches, J. Maric, H. Thunman, P. Knutsson, M. Seemann, Development of oxygen transport properties by olivine and feldspar in industrial-scale dual fluidized bed gasification of woody biomass, Energy Fuel 35 (2021), https://doi.org/10.1021/acs.energyfuels.1c00586.

[43] S. Pissot, H. Thunman, P. Samuelsson, M. Seemann, Production of negative-emissions steel using a reducing gas derived from dfb gasification, Energies (basel) 14 (2021), https://doi.org/10.3390/en14164835.

[44] M. Israelsson, A. Larsson, H. Thunman, Online measurement of elemental yields, oxygen transport, condensable compounds, and heating values in gasification systems, Energy Fuel 28 (2014), https://doi.org/10.1021/ef501433n.

[45] C. Mandviwala, R. Forero Franco, I. Gogolev, J. González-Arias, T. Berdugo Vilches, I.C. Cañete Vela, H. Thunman, M. Seemann, Method development and evaluation of product gas mixture from a semi-industrial scale fluidized bed steam cracker with GC-VUV, Fuel Processing Technology 253 (2024). https://doi.org/10.1016/j.fuproc.2023.108030.

[46] M.N. Dunkle, P. Pijcke, W.L. Winniford, M. Ruitenbeek, G. Bellos, Method development and evaluation of pyrolysis oils from mixed waste plastic by GC-VUV, J. Chromatogr. A 1637 (2021), https://doi.org/10.1016/j.chroma.2020.461837.

[47] R. Forero-Franco, I. Cañete-Vela, T. Berdugo-Vilches, J. González-Arias, J. Maric, H. Thunman, M. Seemann, Correlations between product distribution and feedstock composition in thermal cracking processes for mixed plastic waste, Fuel 341 (2023), https://doi.org/10.1016/j.fuel.2023.127660.

[48] K.M. Van Geem, M.F. Reyniers, G.B. Marin, Two severity indices for scale-up of steam cracking coils, Ind. Eng. Chem. Res. 44 (2005), https://doi.org/10.1021/ie048988j.

[49] K. Barazandeh, O. Dehghani, M. Hamidi, E. Aryafard, M.R. Rahimpour, Investigation of coil outlet temperature effect on the performance of naphtha cracking furnace, Chem. Eng. Res. Des. 94 (2015), https://doi.org/10.1016/j.cherd.2014.08.010.

[50] S.P. Pyl, T. Dijkmans, J.M. Antonykutty, M.F. Reyniers, A. Harlin, K.M. Van Geem, G.B. Marin, Wood-derived olefins by steam cracking of hydrodeoxygenated tall oils, Bioresour. Technol. (2012), https://doi.org/10.1016/j.biortech.2012.09.037.

[51] E. Hájeková, B. Mlynková, M. Bajus, L. Špodová, Copyrolysis of naphtha with polyalkene cracking products; the influence of polyalkene mixtures composition on product distribution, J. Anal. Appl. Pyrol. 79 (2007), https://doi.org/10.1016/j.jaap.2006.12.022.

[52] M. Kusenberg, M. Roosen, A. Zayoud, M.R. Djokic, S. Dao Thi, S. De Meester, K. Ragaert, U. Kresovic, K.m. Van Geem, Assessing the feasibility of chemical recycling via steam cracking of untreated plastic waste pyrolysis oils: Feedstock impurities, product yields and coke formation, Waste Manage. 141 (2022), https://doi.org/10.1016/j.wasman.2022.01.033.

[53] W. Kaminsky, Chemical recycling of plastics by fluidized bed pyrolysis, Fuel Commun. 8 (2021), https://doi.org/10.1016/j.jfueco.2021.100023.

[54] S.H. Jung, M.H. Cho, B.S. Kang, J.S. Kim, Pyrolysis of a fraction of waste polypropylene and polyethylene for the recovery of BTX aromatics using a fluidized bed reactor, Fuel Process. Technol. 91 (2010), https://doi.org/10.1016/j.fuproc.2009.10.009.

[55] P. Tian, Y. Wei, M. Ye, Z. Liu, Methanol to olefins (MTO): From fundamentals to commercialization, ACS Catal. 5 (2015), https://doi.org/10.1021/acscatal.5b00007.

[56] H.F. Joaquin, L. Juan, Quantification of poisons for Ziegler Natta catalysts and effects on the production of polypropylene by gas chromatographic with simultaneous detection: Pulsed discharge helium ionization, mass spectrometry and flame ionization, J. Chromatogr. A 1614 (2020), https://doi.org/10.1016/j.chroma.2019.460736.